Clathrin-mediated endocytosis is inhibited during mitosis

Andrew B. Fielding, Anna K. Willox, Emmanuel Okeke, and Stephen J. Royle[1]

Department of Cellular and Molecular Physiology, Institute of Translational Medicine, University of Liverpool, Liverpool L69 3BX, United Kingdom

Edited by David D. Sabatini, New York University School of Medicine, New York, NY, and approved March 15, 2012 (received for review October 21, 2011)

A long-standing paradigm in cell biology is the shutdown of endocytosis during mitosis. There is consensus that transferrin uptake is inhibited after entry into prophase and that it resumes in telophase. A recent study proposed that endocytosis is continuous throughout the cell cycle and that the observed inhibition of transferrin uptake is due to a decrease in available transferrin receptor at the cell surface, and not to a shutdown of endocytosis. This challenge to the established view is gradually becoming accepted. Because of this controversy, we revisited the question of endocytic activity during mitosis. Using an antibody uptake assay and controlling for potential changes in surface receptor density, we demonstrate the strong inhibition of endocytosis in mitosis of CD8 chimeras containing any of the three major internalization motifs for clathrin-mediated endocytosis (YXXΦ, [DE]XXXL[LI], or FXNPXY) or a CD8 protein with the cytoplasmic tail of the cation-independent mannose 6-phosphate receptor. The shutdown is not gradual: We describe a binary switch from endocytosis being "on" in interphase to "off" in mitosis as cells traverse the G_2/M checkpoint. In addition, we show that the inhibition of transferrin uptake in mitosis occurs despite abundant transferrin receptor at the surface of HeLa cells. Our study finds no support for the recent idea that endocytosis continues during mitosis, and we conclude that endocytosis is temporarily shutdown during early mitosis.

cell division | moonlighting | receptor trafficking | endosomal recycling | prometaphase

Clathrin-mediated endocytosis (CME) is important for diverse processes such as cell signaling, nutrient uptake, and cell motility (1). Receptors destined for CME become concentrated in clathrin-coated pits at the cell surface where they bind to adaptor proteins and, hence, clathrin via specific endocytic motifs present in their cytoplasmic tails (2).

A long-standing tenet in cell biology is the shutdown of endocytosis during mitosis. Nearly 50 years ago, the separation of ferritin-containing coated vesicles from the plasma membrane was found to be inhibited during cell division (3). Subsequently, suppression of a broad range of endocytic processes was observed during mitosis (4). Quantification of this phenomenon revealed a 30-fold decrease in fluid-phase endocytosis, a process that is largely attributable to CME (5), which occurred within 30 s of entry into prophase (6). Further studies demonstrated that uptake of fluorescent dextran ceases during mitosis and also confirmed the timing of shutdown to be in early prophase (7). Many other studies went on to confirm and further develop the theory of mitotic shutdown of endocytosis, showing that it is temporary and resumes in telophase (8–17). The reason for shutdown is unclear (18, 19), but one recent idea is that "moonlighting" functions for endocytic proteins during mitosis may contribute to the inhibition (20, 21).

Despite this wealth of evidence, a recent report suggested that CME is, in fact, normal throughout all phases of cell division (22). The authors suggested that the amount of plasma membrane decreases at the beginning of mitosis and then increases during anaphase and telophase, with complete recovery before abscission (22, 23). It was proposed that this phenomenon could occur if CME is continuous throughout cell division, whereas recycling of internalized membranes back to the cell surface is slowed considerably at the beginning of mitosis and reactivated in anaphase, leading to plasma membrane recovery (22). What made this study so compelling was that it argued that previous results describing endocytic shutdown had been misinterpreted. For example, as in many other studies, the authors described a reduction in transferrin uptake in mitotic cells, being lowest at metaphase (22). However, measurements of surface-bound transferrin showed an even larger decrease indicating that the endocytic rate is actually increased, not decreased, during mitosis (22). It was suggested that the relative amount of receptors at the surface had not been accounted for, leading to a misinterpretation of the results. In addition, a recent report using a similar methodology showed an increase in endocytosis of some, but not all, chimeric myc-tagged TGF-β type I receptors during mitosis (24). Despite relatively little evidence, the idea that endocytosis is continuous throughout mitosis seems to be becoming established (21, 25–27).

Because of this controversy, we set out to reexamine endocytosis during cell division. Because transferrin receptor (TfR) surface levels may vary between different stages of the cell cycle (7, 22) and also between different cell lines (7), transferrin uptake measurements may be difficult to interpret. We therefore used an alternative reporter of CME, the CD8 chimera system (28–30). We found that endocytosis is severely reduced during mitosis for all of the endocytic motifs examined, with cells rapidly transitioning from possessing full endocytic activity to only minimal levels as cells go into mitosis. We also show that, in HeLa cells, transferrin uptake is severely reduced despite surface receptor levels remaining normal throughout mitosis. Our results argue that the theory of endocytic shutdown during mitosis is correct.

Results

Endocytosis Is Strongly Inhibited During Mitosis. To characterize the endocytosis of proteins with a range of important endocytic motifs, we used the well-described CD8 chimera system (28–31). This system comprises a set of constructs, each with the extracellular and transmembrane domain of CD8 α-chain, with varying cytosolic domains. Briefly, CD8 WT (CD8-WT) contains no known sorting signals in its cytoplasmic tail, is therefore not subject to endocytosis and is resident at the plasma membrane (28). CD8-cation–independent mannose 6-phosphate receptor (CIMPR) contains the cytoplasmic domain of CIMPR, a well-characterized cargo that is efficiently internalized in clathrin-coated vesicles before being trafficked to the *trans*-Golgi network (TGN) and a subset of late endosomes, via sorting and recycling endosomes (32, 33). The remaining constructs contain "designer" tails that represent three well-established endocytic motifs: YXXΦ (CD8-YAAL), [DE]XXXL[LI] (CD8-EAAALL), and FXNPXY (CD8-FANPAY), all transposed on a background of eight alanines (CD8-8xA) (28). To study endocytosis in mitotic cells, we first used a flow cytometry-based antibody uptake assay that allowed us to

Author contributions: S.J.R. designed research; A.B.F., A.K.W., and E.O. performed research; A.B.F. and A.K.W. analyzed data; and A.B.F. and S.J.R. wrote the paper.

The authors declare no conflict of interest.

This article is a PNAS Direct Submission.

[1]To whom correspondence should be addressed. E-mail: s.j.royle@liverpool.ac.uk.

This article contains supporting information online at www.pnas.org/lookup/suppl/doi:10.1073/pnas.1117401109/-/DCSupplemental.

monitor the surface population of CD8 to control for any changes that may occur (Fig. 1*A*).

In this assay, cells are incubated with Alexa488-conjugated anti-CD8 at 37 °C for 40 min to label any CD8 that is internalized in this time. Cells are then shifted to 4 °C to prevent uptake, and plasma membrane CD8 fluorescence is first quenched with an anti-Alexa488 antibody and then relabeled with an anti-mouse Alexa633 antibody before fixation and analysis by flow cytometry (28). Thus, measuring green fluorescence from cells displaying similar far-red fluorescence (surface) allows quantification of internalized CD8 (Fig. 1*A*).

Cells transfected with the set of CD8 constructs were synchronized at various stages of the cell cycle; in interphase by arresting in S phase using thymidine, at the G_2/M checkpoint using RO-3306 (34), or in mitosis by 30-min release from RO-3306 or arrest using nocodazole. In addition, hypertonic sucrose, which inhibits endocytosis (35), was used as a control to represent endocytic block. Fig. 1*B* shows example flow cytometry plots of interphase (thymidine treated), mitotic (RO-3306, 30-min release), and sucrose-treated interphase cells. Under all conditions, CD8-WT and CD8-8xA display the same profile, with cells expressing CD8 at their surface and showing essentially no uptake of CD8 (Fig. 1*B*). Cells expressing higher amounts of CD8-WT or CD8-8xA at the surface show some green fluorescence, which is probably due to inefficient quenching of surface anti–CD8-Alexa488 (28). Cells in interphase expressing CD8 chimeras with internalization motifs display a markedly different profile (Fig. 1*B, Top*). In these cells, high levels of internalized fluorescence are apparent at moderate levels of surface expression, indicating CME. By contrast, cells in mitosis expressing CD8 chimeras containing endocytic motifs display a similar distribution as CD-WT or CD8-8xA cells (Fig. 1*B, Middle*), with very little internalization. These profiles can be compared with those from interphase cells where endocytosis has been inhibited using hypertonic sucrose (Fig. 1*B, Bottom*). This result indicates endocytosis of these constructs is strongly inhibited during mitosis.

To quantify these data, events were gated to select cells expressing similar, moderate surface CD8 levels (Fig. 1*C*), as described (28). Antibody uptake, normalized to CD8-YAAL expressing, thymidine-arrested cells, was then plotted for each of the constructs (Fig. 1*D*). As expected, in interphase, cells expressing constructs with internalization motifs showed robust internalization compared with CD8-WT and CD8-8xA. However, mitotic cells showed an essentially complete inhibition of internalization, because the average green fluorescence was reduced to the same levels as CD-WT or CD8-8xA (Fig. 1*D*).

Endocytic Shutdown in Mitosis Is a Binary Event. Although mitotic cells showed an inhibition of internalization down to CD8-WT or CD8-8xA levels, it was noted that cells treated with, but not released from, RO-3306 before the antibody uptake assay (RO-3306 no release) showed uptake but that it was significantly lower than cells in S phase (Fig. 1*D*). This observation could mean that cells at the G_2/M boundary show a reduced but not complete inhibition of mitosis, perhaps suggesting a slowing down of endocytosis as cells approach mitosis. Alternatively, these data could be explained by

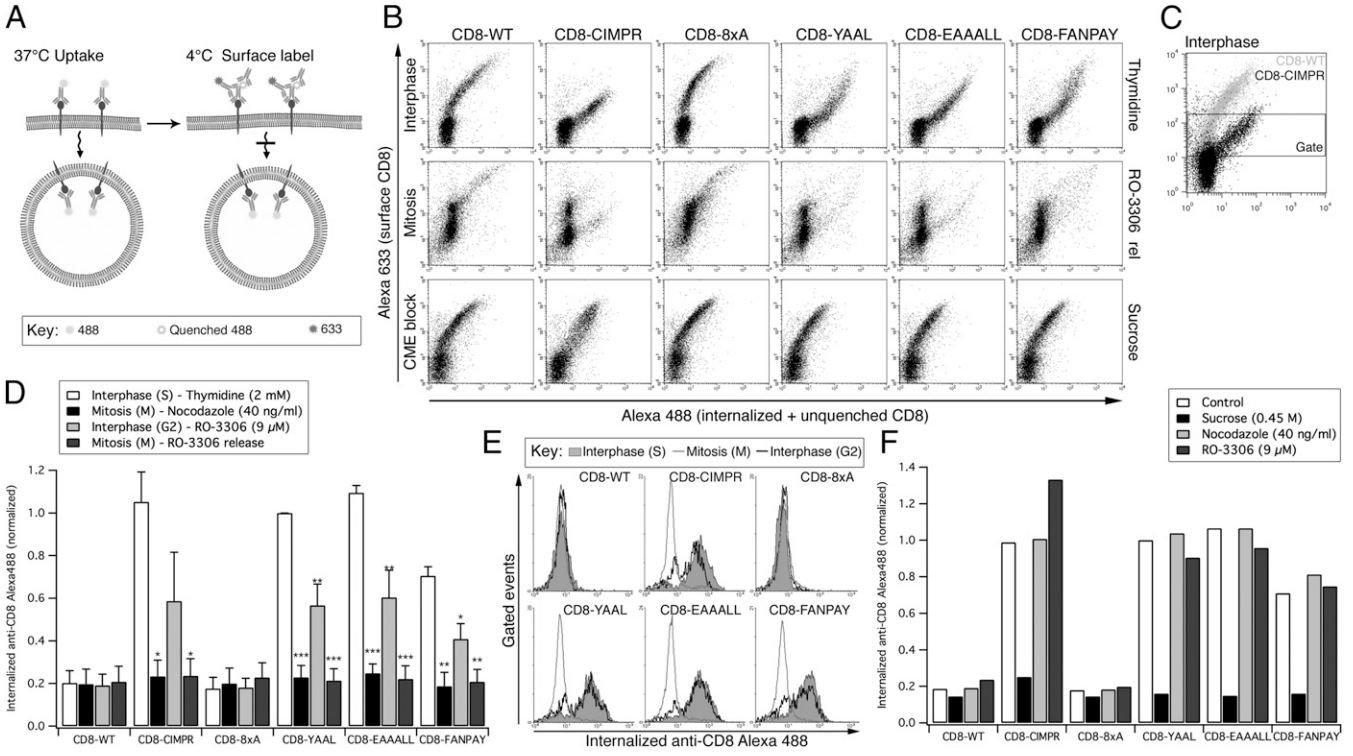

Fig. 1. Internalization of CD8 chimeras is strongly inhibited in mitosis. (*A*) Schematic representation of flow-cytometry based antibody uptake assay (28). (*B*) Representative flow cytometry plots of internalized (anti–CD8-Alexa488, *x* axis) versus surface CD8 (anti–Alexa488-Alexa633, *y* axis). Examples are shown from cells in interphase (S phase, 2 mM thymidine), mitosis (9 μM RO-3306, 30-min release), or interphase with inhibition of CME (S phase + 0.45 M sucrose). Note that there are fewer mitotic cells with very low surface amounts of CD8, but that these lie outside the gate. (*C*) Illustration of the gating procedure to analyze cells expressing moderate levels of CD8 at the cell surface. (*D*) Quantification of flow cytometry experiments. Signals were gated to analyze the internalization in cells expressing moderate amounts of CD8 at the cell surface. The geometric mean amount of internalized anti–CD8-Alexa488 was normalized to thymidine-treated CD8-YAAL uptake. Mean ± SEM of three independent experiments plotted as a bar graph. $^*P < 0.05$, $^{**}P < 0.01$, and $^{***}P < 0.001$. (*E*) Antibody uptake profiles for interphase (2 mM thymidine), G_2/M border (9 μM RO-3306 with no release) and mitosis (9 μM RO-3306, 30-min release). Gated events are shown as overlaid histograms of internalized anti–CD8-Alexa488 fluorescence (*x* axis) against the number of events (*y* axis). (*F*) Bar chart to summarize a typical antibody uptake experiment to test for direct effects of nocodazole and RO-3306 on CME. Cells were released from a thymidine block and the anti–CD8-Alexa488 uptake assay performed in the presence of nocodazole, RO-3306 or sucrose.

the presence of a mixed population of cells in this sample, each displaying a binary response but averaging out to an intermediate reading. This possibility could be accounted for by the release of a portion of the cells from the G_2/M block into mitosis during the time course of the antibody uptake assay. To investigate this observation, the gated flow cytometry events for thymidine and RO-3306 0- or 30-min release were plotted as histograms for comparison (Fig. 1*E*). In CD8-WT or CD8-8xA cells, the same single peak is observed in all three conditions, indicating no uptake regardless of cell cycle stage. In thymidine-treated cells expressing CD8-CIMPR, CD8-YAAL, CD8-EAAALL, and CD8-FANPAY, a single peak at high green fluorescence intensity is observed, representing internalized CD8. At 30-min release from RO-3306, this peak is shifted to the left, indicating the inhibition of endocytosis. However, the RO-3306 0-min release shows two distinct peaks, one overlaying with the thymidine peak and the second with the 30-min release from RO-3306 peak (Fig. 1*E*). This result indicates that this sample is a mixed population of cells, each showing binary responses, and the observed decrease in Fig. 1*D* was not due to partial endocytic shutdown in late G_2, but rather the average result of a sample containing cells at the G_2/M border with interphase levels of endocytosis and a mitotic population with inhibited endocytosis. We interpret this result to mean that endocytosis is under binary control by the cell cycle: It is either on in interphase or off during early mitosis.

We next tested whether the observed inhibition of endocytosis was due to the stage in the cell cycle or if the drugs used for synchronization caused the observed endocytic defects. Accordingly, we transiently treated interphase-synchronized cells with either nocodazole or RO-3306 and performed the antibody uptake assay (Fig. 1*F*). Internalization of the CD8 constructs was not affected by transient treatment with either nocodazole or RO-3306, demonstrating that the effects observed in Fig. 1*D* were due to the cell cycle stage of the cells and not an effect of the small molecules per se.

Mitotic Inhibition of Endocytosis Was Confirmed Using Fluorescence Microscopy. The flow cytometry assay of CD8 trafficking was carried out on synchronized cells in suspension. To verify our observations, we next used the same labeling protocol (Fig. 1*A*) on asynchronous HeLa cells grown on coverslips and visualized the cells by confocal microscopy. Internalization was evident at interphase for CD8-CIMPR, CD8-YAAL, CD8-EAAALL, and CD8-FANPAY, but not for CD8-WT and CD8-8xA (Fig. 2*A*). In mitosis, virtually no internalization was seen for any CD8 construct. In all conditions, good surface expression was detected (Fig. 2*A* and Fig. S1). These data confirm that there is no appreciable uptake of CD8 constructs in mitotic cells.

So far, our CD8 experiments were carried out with a single labeling time point (40 min). It is possible, but rather unlikely, that internalization can occur, but it is not detected because of rapid recycling. To visualize whether internalization occurs at all, we imaged living HeLa cells expressing the CD8 constructs and applied Alexa488-conjugated anti-CD8 to monitor endocytosis. Again, uptake was seen for CD8 constructs with internalization signals during interphase but not during early mitosis. Example frames from these experiments are shown for CD8-YAAL and CD8-FANPAY (Fig. 2*B*). CD8 at the cell surface was intensely stained during this procedure, indicating that the lack of internalization was due to inhibition of endocytosis and not due to problems in surface labeling.

To further verify our results, we next determined the steady-state subcellular localization of the transfected CD8 chimeric constructs in interphase and mitotic cells (Fig. 2*C*). Cells were fixed, permeabilized, and stained with the Alexa488-conjugated anti-CD8 antibody and 4′,6-diamidino-2-phenylindole (DAPI). The localization of all of the constructs in interphase recapitulated the results of the antibody uptake experiments. CD8-WT and CD8-8xA were almost exclusively localized at the plasma membrane, whereas CD8-CIMPR, CD8-YAAL, CD8-EAAALL, and CD8-FANPAY were all resident in intracellular puncta and/or perinuclear compartments, with little plasma membrane staining.

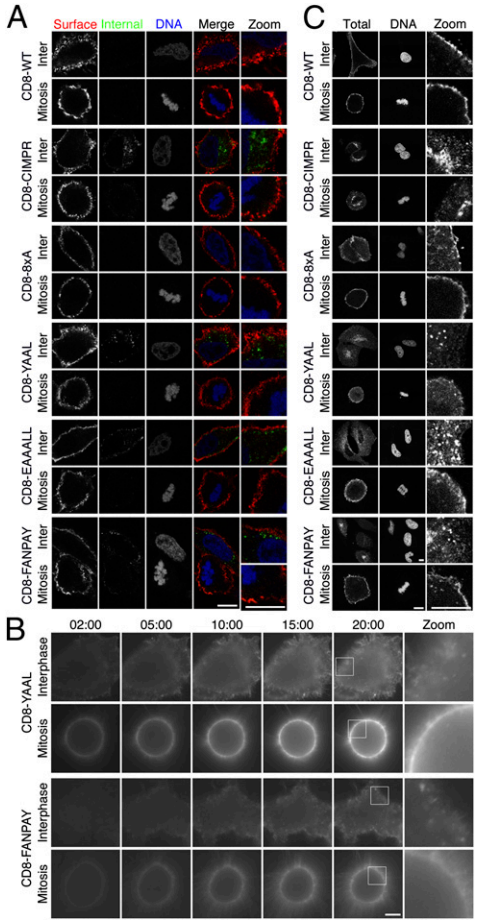

Fig. 2. CD8 chimeras endowed with internalization motifs are predominantly localized to the plasma membrane and are not internalized during mitosis. (*A*) Representative confocal images of anti-CD8 antibody uptake experiments. Uptake was performed as described in Fig. 1*A*. Internalized CD8 is shown in green, and surface CD8 is shown in red. 3D reconstructions of these cells are shown in Fig. S1. (*B*) Live cell imaging of Alexa488-conjugated anti-CD8 uptake in cells expressing CD8-YAAL or CD-FANPAY. Note the extensive membrane labeling in mitotic cells. (C) Representative confocal images of the subcellular distribution of CD8 constructs in permeabilized HeLa cells at interphase or mitosis. Each row of images shows anti-CD8 and DAPI staining of permeabilized interphase and mitotic cells expressing the indicated chimeras. (Scale bars: 10 μm.)

However, in mitotic cells, CD8-YAAL, CD8-EAAALL, and CD8-FANPAY were now predominately localized at the plasma membrane, with little intracellular fluorescence. The CD8-CIMPR chimera had a substantial intracellular pool in mitotic cells. This pool is likely due to different trafficking routes. Although proteins containing YXXΦ, [D/E]XXXL[L/I], or FXNPXY motifs typically show rapid recycling back to the plasma membrane after internalization, a proportion of CIMPR also traffics to the TGN and late endosomes (33). Recycling from here to the plasma membrane will necessarily take more time. Therefore, intracellular CD8-CIMPR that is present in mitotic cells was probably internalized before mitotic entry. Taken together, these results suggest that the dynamics of clathrin-coated vesicle internalization are dramatically altered during mitosis. Moreover, they confirm that the lack of CD8 uptake in mitosis is due to endocytic shutdown and not due to a decrease of the population of receptors at the plasma membrane, as argued (22).

Transferrin Uptake Is Reduced in Mitotic Cells Despite Abundant Surface TfR. There is consensus that transferrin uptake is inhibited during mitosis (for example, refs. 11, 15, 22, 36, and 37).

However, it was contended recently that this inhibition is not due to endocytic shutdown but is instead due to a reduction in TfRs at the surface (22). We next investigated the internalization of endogenous TfRs in HeLa cells during interphase and mitosis. First, we measured by flow cytometry the uptake of Alexa488-conjugated transferrin in synchronized HeLa cells (Fig. 3*A*). These experiments once again confirmed that uptake of transferrin is inhibited during mitosis. Second, the uptake of Alexa488 transferrin was followed by labeling of surface TfRs with Alexa647 transferrin at 4 °C. Here, mitotic cells showed similar surface labeling to interphase cells suggesting that the lack of uptake during mitosis is not due to a decrease in TfRs at the cell surface (Fig. S2). To confirm these observations by an alternative approach, we labeled the endogenous TfR by using a similar protocol to that used for the CD8 experiments (*Materials and Methods*). In these experiments, the ratio of labeled TfRs that were internalized versus those on the surface was decreased significantly in mitotic cells compared with those in interphase (Fig. 3*B*). This ratio was comparable to blockade of CME in interphase cells by using hypertonic sucrose. Importantly, the level of TfR at the surface of mitotic cells was not reduced compared with interphase cells, as suggested (Fig. 3*C*).

Inhibition of TfR Endocytosis During Early Mitosis Observed Using Fluorescence Microscopy. We next verified our flow cytometry measurements of TfR trafficking by using asynchronous HeLa cells on coverslips and confocal microscopy. Cells were incubated with Alexa488-labeled transferrin at 4 °C before being shifted to 37 °C for 7 min to allow potential uptake. Cells were then acid-washed to remove surface-bound transferrin before fixation and subsequent staining with anti-TfR antibody, without cell permeabilization. Full *Z*-series of interphase or mitotic cells were captured, and the total fluorescence was quantified (Fig. 4*A*). The amount of internalized transferrin was significantly reduced in mitotic cells compared with those in interphase, whereas the amount of surface TfR was significantly increased. Again, we found that the ratio of internalized transferrin versus the surface TfR was significantly reduced during mitosis (Fig. 4*A Inset*). Once more, these experiments verify that the inhibition of transferrin uptake seen during mitosis by all investigators is not due to a reduction in TfRs at the cell surface.

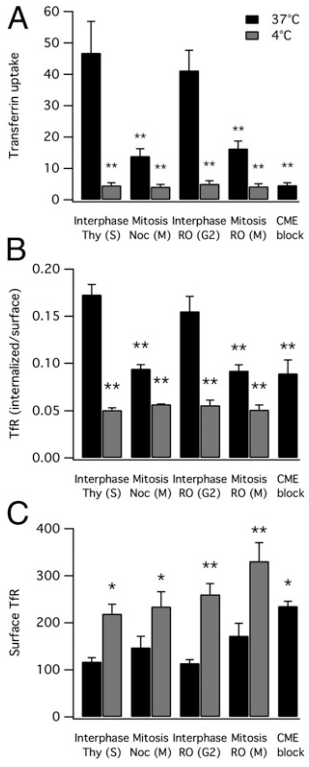

Fig. 3. Transferrin uptake and endocytosis of endogenous transferrin receptors (TfRs) is inhibited during mitosis despite abundant surface TfR. Summary bar charts of flow cytometry experiments to test the effect of cell cycle stage on uptake of Alexa488-conjugated transferrin (*A*), the ratio of internalized to surface labeled TfR (*B*), and the abundance of TfR at the cell surface (*C*). Data are mean ± SEM of at least three independent experiments. $*P < 0.05$, $**P < 0.01$.

To examine the mitotic shutdown of endocytosis and its subsequent recovery, cells were labeled as above and imaged at different stages of mitosis. Fig. 4*B* and Fig. S3 show that although transferrin was readily internalized in interphase cells, prometaphase, metaphase, and anaphase cells displayed a marked decrease in uptake. However, in the same cells, TfR staining remained abundant at the cell surface throughout all stages of cell division, being at least as pronounced as in neighboring interphase cells visible in the same field. This experiment suggests that, in HeLa cells, TfR availability at the cell surface cannot be a limiting factor for endocytosis at any stage of the cell cycle. In cells that have progressed to telophase and cytokinesis, robust uptake is apparent (Fig. 4*B*). These data indicate that the mitotic shutdown of endocytosis occurs during early mitosis, peaking at prometaphase and metaphase.

How is CME shut down during early mitosis? CME is a multistep pathway, and so we looked at what stage the process might be inhibited to inform future work. The colocalization of TfRs and clathrin was assessed in mitotic cells by using confocal microscopy. TfRs at the cell surface could clearly be seen to colocalize with clathrin puncta (Fig. 4*C*). These puncta likely correspond to clathrin-coated pits that are arrested (8). These observations suggest that the inhibition occurs at a comparatively late stage of CME. Receptors on the surface of mitotic cells are able to engage adaptors and to concentrate in pits but that the invagination and/or progression of pits into vesicles is inhibited specifically.

Having confirmed that CME is shut down during mitosis, we wondered whether this regulation is specific to CME or whether all forms of constitutive endocytosis are inhibited. Accordingly, we labeled the plasma membrane of live cells by using 15 μM FM4-64 for 10 min. Excess dye was washed from the plasma membrane with constant perfusion for 10 min, and any uptake of labeled membrane was then visualized by fluorescence microscopy (Fig. 4*D*). In interphase cells, many bright puncta were observed, suggesting robust internalization of plasma membrane. By contrast, neighboring mitotic cells showed very few, if any, intracellular puncta, indicating that general uptake of plasma membrane is substantially decreased in mitotic cells. These experiments provide a further indication of reduced endocytic activity during mitosis. In addition, this assay is independent of receptor availability at the plasma membrane and suggests that all forms of constitutive endocytosis are shut down during mitosis.

Discussion

A long-established concept in cell biology is the shutdown of endocytosis during mitosis (for reviews, see refs. 18 and 38). However, this idea was challenged recently by two studies that reported endocytosis to be normal throughout all phases of cell division (22, 24). These studies argued that because potential changes in surface receptor number may not have been controlled for, previous work showing that uptake was inhibited during mitosis could have been misinterpreted (22). This argument was compelling, and a new view—that endocytosis continues during mitosis—was fast becoming established (21, 25–27).

Here, we revisited this question by using a variety of approaches and found no evidence for continued endocytosis during mitosis. Our methods allowed us to monitor the number of receptors at the cell surface, and we did not detect a decrease during early mitosis. If anything, the number of receptors at the surface of mitotic cells may actually be increased, and so it is highly unlikely that the mitotic inhibition of uptake, which is undisputed, is due to unavailability of receptors at the cell surface. Instead, our results, supported by de-

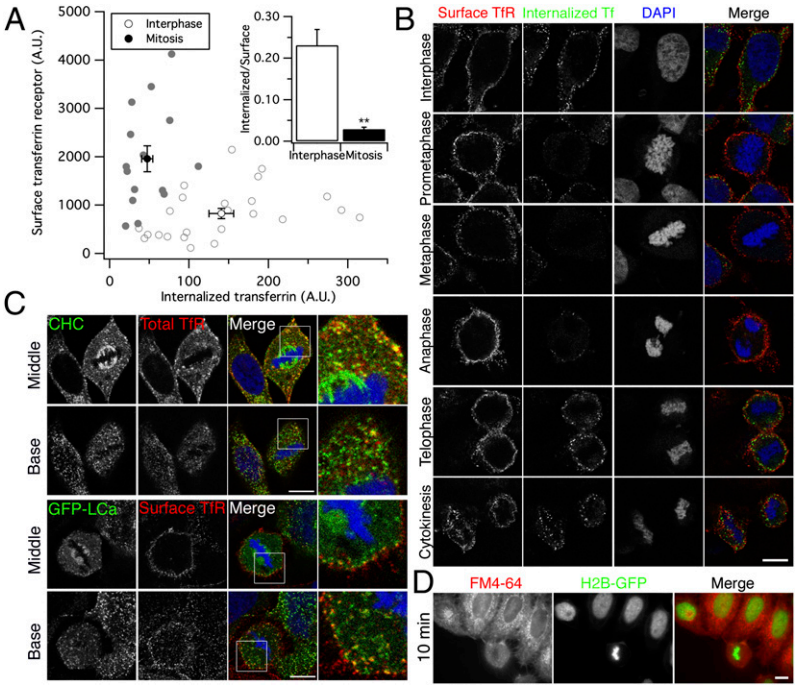

Fig. 4. Transferrin uptake is inhibited during early mitosis despite abundant surface TfR. (*A*) Quantification of transferrin uptake and surface TfR from whole-cell confocal images. A plot of values from 24 interphase cells (white) and 15 cells in early mitosis (gray), mean ± SEM for all cells is indicated. *Inset* shows the mean ± SEM ratio of transferrin uptake to surface TfR. (*B*) Representative confocal images of HeLa cells after 7-min uptake of Alexa488-conjugated transferrin at 37 °C. Cells were acid-washed to remove surface-bound transferrin, fixed, and stained by using anti-TfR antibody. Images of cells at different stages of mitosis are shown. Note the recovery of internalization that begins in anaphase. 3D reconstructions of *Z*-series confocal images are shown in Fig. S3. (*C*) Representative confocal images to show colocalization of clathrin and TfR in the middle or base of a mitotic cell. Clathrin is detected by staining with anti-clathrin heavy chain (CHC; *Upper*) or by expression of GFP-tagged clathrin light chain a (GFP-LCa; *Lower*). Total TfR or TfR at the surface in nonpermeabilized cells are as indicated. Threefold zoomed panels are shown (*Right*). (*D*) Representative fluorescence micrograph from experiments to examine uptake of FM4-64-labeled plasma membrane in HeLa cells. H2B-GFP expressing HeLa cells were incubated with FM4-64 for 10 min and live-cell imaging performed as described (*Materials and Methods*). (Scale bars: 10 μm.)

cades of previous work, point definitively to a direct inhibition of the process of endocytosis during early mitosis.

We initially used the CD8 reporter system and flow cytometry, which allowed us to control for the surface population of receptors and only analyze cells with similar, moderate amounts of CD8 at the cell surface. In brief, we found that CD8-CIMPR or CD8 constructs with any one of three endocytic motifs (YXXΦ, [D/E]XXXL[L/I], or FXNPXY) were internalized during interphase but not during early mitosis. In fact, mitotic uptake of these proteins was comparable to that of CD8-WT or CD8-8xA, which are unable to be internalized. Moreover, the degree of shutdown was similar to inhibition of endocytosis in interphase cells by using hypertonic sucrose treatment (35). Similar results were obtained by microscopy using adherent cells that were growing asynchronously. In fact, the subcellular distributions of the CD8 constructs indicated that a large proportion of the CD8 chimeras that contain endocytic motifs was localized at the plasma membrane at steady-state during mitosis, again indicating that endocytosis is shut down during mitosis.

Analysis of the dynamics of endocytic shutdown revealed that CME is, at least with our temporal resolution, essentially a binary event. It is at normal levels at the end of G_2, yet completely inhibited during early mitosis. This observation supports previous work that described endocytic shutdown occurring rapidly after cells enter prophase (6, 7). The speed at which endocytosis decreases does not support the hypothesis that membrane area could be reduced by 50% or more as cells enter mitosis (22). As the cell rounds up on mitotic entry, the cytoplasmic volume is decreased (23, 39, 40), but there is not a clear consensus on any change in the surface area of the plasma membrane. Several studies have variously reported a decrease (22), an increase (41), or no change in cell surface area (39, 42, 43). Accurate measurement of cell surface area by low-resolution light microscopy (22) is not straightforward because the plasma membrane in mitotic cells is puckered (39, 42, 43). Interestingly, our live cell anti-CD8 labeling experiments (Fig. 2*B*) highlighted the significant amount of plasma membrane surrounding the retraction fibers that hold the cell to the coverslip (44). We speculate that this membrane may not have been accounted for in previous work (22). Cell rounding in mitosis is primarily driven by osmotic changes with a contribution by the actomyosin cell cortex (40). Although the later stages of cell division (e.g., cytokinesis) clearly involve massive membrane remodeling, this situation need not be the case in early mitosis when endocytosis is shut down.

To further confirm the shutdown of endocytosis during early mitosis, we also tested the endogenous TfR. As expected, the receptor, which contains a YXXΦ sorting motif was regulated in the same way as the CD8-YAAL reporter. Our transferrin uptake experiments confirmed many previous reports of reduced transferrin uptake during mitosis (7, 11, 15, 22, 36, 37). Staining of surface TfR indicated that it was abundant at the cell surface during all stages of the cell cycle in HeLa cells. Mitotic A431 cells display reduced staining of TfR at the cell surface compared with interphase cells, although the same study reported a less marked reduction in HeLa cells (7). The availability of TfR at the surface of HeLa cells indicates that the observed decrease in transferrin uptake is not due to a lack of TfR in this cell type, as suggested (22). Therefore, the most likely explanation of this result is a decrease in endocytosis during prometaphase, metaphase, and anaphase (7, 15).

What seems clear from this study and the many preceding it, is that constitutive endocytosis is definitely inhibited during early mitosis. So are there any cases where endocytosis can occur during mitosis? In some specialized cases, there is good evidence for an override mechanism. For example, the atypical cadherin Celsr1, which is internalized to maintain an asymmetric distribution at the plasma membrane (45). This protein uses a dileucine sorting motif for internalization, and this phenomenon seems to be particular to this planar cell polarity component. Another example is the epidermal growth factor receptor (EGFR), which can be internalized in mitotic cells in a ligand-dependent manner, albeit after a long delay (37). In contrast to EGFR internalization in interphase cells, mitotic uptake of EGFR was shown to be kinase-dependent and clathrin-independent (37). Although the nature of potential override mechanisms needs further investigation, this work should follow on from the more fundamental question of how and why constitutive endocytosis is halted during cell division; a full molecular picture of which still remains to be elucidated. Understanding how the cell regulates constitutive endocytosis is important because if mitotic shutdown can be mimicked pharmacologically in interphase cells, infection of cells by pathogens using this entry pathway may be preventable.

Materials and Methods

Cell Culture and Reagents. HeLa cells were grown in DMEM containing 10% (vol/vol) FBS and penicillin/streptomycin at 37 °C/5% CO_2. CD8 chimera cDNA constructs (28) were a kind gift from Scottie Robinson (University of Cambridge, Cambridge, United Kingdom). H2B-GFP, H2B-mCherry, and GFP-LCa were available from previous work (36).

Flow Cytometry. Analysis of surface and internalized CD8 was performed as described (28). HeLa cells expressing CD8 constructs were synchronized in S phase with 2 mM thymidine for 18 h, at the G_2/M checkpoint with 9 μM RO-3306 for 18 h (34) and in M-phase either by 30-min release from RO-3306 treatment or with 40 ng/mL nocodazole for 16 h. Thymidine and RO-3306 arrested cells were trypsinized, whereas cells in mitosis (nocodazole-arrested or those released for 30 min from RO-3306 block) were gently isolated by shake-off. For endocytic block, interphase (thymidine) cells were incubated with hypertonic sucrose (0.45 M) during the uptake assay (35).

For analysis of transferrin uptake, synchronized cells were suspended, serum-starved for 30 min, then incubated with 50 μg/mL Alexa488-conjugated transferrin for 5 min at 4 °C, then moved to 37 °C and incubated for 10 min. Cells were pelleted, washed in ice cold 1% BSA/PBS, acid-washed twice, and fixed before flow cytometric analysis.

Analysis of internalized and surface TfR was performed by using a similar method to CD8 labeling. For each sample, 1×10^4 events were acquired and geometric means with no gating (or $>1 \times 10^3$ events after gating for CD8 experiments) from three independent experiments were used for comparison.

Immunofluorescence and Live-Cell Labeling. Immunofluorescence was as described (36), before mounting in Mowiol containing 10 μg/mL DAPI. For immunofluorescence analysis of the CD8 uptake assay, asynchronous HeLa cells on coverslips were labeled as above, except Alexa568-conjugated anti-mouse IgG secondary was used to label the surface CD8.

For live-cell imaging of CD8 uptake, cells were synchronized by using RO-3306 as above, released for 25 min then transferred to CO_2-independent media and a 37 °C, humidified microscope chamber. Cells in prometaphase or metaphase were identified by H2B-mCherry. Alexa488-conjugated anti-CD8 antibody was then added at 1:100 dilution in CO_2-independent media, and images were acquired every 30 s for 30 min.

For transferrin uptake experiments, the cells were serum-starved for 45 min at 37 °C in DMEM. Cells were incubated on ice for 5 min followed by addition of 50 μg/mL Alexa488-conjugated transferrin (Invitrogen) in DMEM. After 30 min on ice, cells were transferred to 37 °C for 7 min, then acid-washed (0.1 M glycine and 150 mM NaCl at pH 3) before fixation (wt/vol 3% paraformaldehyde and 4% sucrose in PBS). Subsequently, cells were stained with rabbit anti-TfR (CBL47; Chemicon) followed by anti-rabbit Alexa568 secondary (1:500, Invitrogen).

For FM4-64 uptake experiments, HeLa cells expressing H2B-GFP were incubated with FM4-64 (15 μM; Invitrogen) for 10 min. Excess dye was washed by using normal extracellular solution (136 mM NaCl, 2.5 mM KCl, 1.3 mM $MgCl_2$, 10 mM Hepes, 2 mM $CaCl_2$, and 10 mM glucose at pH 7.4) for 10 min.

Full details of all methods including microscopy and data analysis are given in *SI Materials and Methods*.

ACKNOWLEDGMENTS. We thank Scottie Robinson for CD8 chimera constructs. This work was supported by Biotechnology and Biological Sciences Research Council Project Grant BB/H015582/1 and by the Wellcome Trust.

1. Brodsky FM, Chen CY, Knuehl C, Towler MC, Wakeham DE (2001) Biological basket weaving: Formation and function of clathrin-coated vesicles. *Annu Rev Cell Dev Biol* 17:517–568.
2. Traub LM (2009) Tickets to ride: Selecting cargo for clathrin-regulated internalization. *Nat Rev Mol Cell Biol* 10:583–596.
3. Fawcett DW (1965) Surface specializations of absorbing cells. *J Histochem Cytochem* 13:75–91.
4. Berlin RD, Oliver JM, Walter RJ (1978) Surface functions during Mitosis I: Phagocytosis, pinocytosis and mobility of surface-bound Con A. *Cell* 15:327–341.
5. Marsh M, Helenius A (1980) Adsorptive endocytosis of Semliki Forest virus. *J Mol Biol* 142:439–454.
6. Berlin RD, Oliver JM (1980) Surface functions during mitosis. II. Quantitation of pinocytosis and kinetic characterization of the mitotic cycle with a new fluorescence technique. *J Cell Biol* 85:660–671.
7. Warren G, Davoust J, Cockcroft A (1984) Recycling of transferrin receptors in A431 cells is inhibited during mitosis. *EMBO J* 3:2217–2225.
8. Pypaert M, Lucocq JM, Warren G (1987) Coated pits in interphase and mitotic A431 cells. *Eur J Cell Biol* 45:23–29.
9. Pypaert M, Mundy D, Souter E, Labbé JC, Warren G (1991) Mitotic cytosol inhibits invagination of coated pits in broken mitotic cells. *J Cell Biol* 114:1159–1166.
10. Oliver JM, Seagrave JC, Pfeiffer JR, Feibig ML, Deanin GG (1985) Surface functions during mitosis in rat basophilic leukemia cells. *J Cell Biol* 101:2156–2166.
11. Sager PR, Brown PA, Berlin RD (1984) Analysis of transferrin recycling in mitotic and interphase HeLa cells by quantitative fluorescence microscopy. *Cell* 39:275–282.
12. Quintart J, Leroy-Houyet MA, Trouet A, Baudhuin P (1979) Endocytosis and chloroquine accumulation during the cell cycle of hepatoma cells in culture. *J Cell Biol* 82:644–653.
13. Illinger D, Italiano L, Beck JP, Waltzinger C, Kuhry JG (1993) Comparative evolution of endocytosis levels and of the cell surface area during the L929 cell cycle: A fluorescence study with TMA-DPH. *Biol Cell* 79:265–268.
14. Woodman PG, Adamczewski JP, Hunt T, Warren G (1993) In vitro fusion of endocytic vesicles is inhibited by cyclin A-cdc2 kinase. *Mol Biol Cell* 4:541–553.
15. Schweitzer JK, Burke EE, Goodson HV, D'Souza-Schorey C (2005) Endocytosis resumes during late mitosis and is required for cytokinesis. *J Biol Chem* 280:41628–41635.
16. Raucher D, Sheetz MP (1999) Membrane expansion increases endocytosis rate during mitosis. *J Cell Biol* 144:497–506.
17. Chen H, Slepnev VI, Di Fiore PP, De Camilli P (1999) The interaction of epsin and Eps15 with the clathrin adaptor AP-2 is inhibited by mitotic phosphorylation and enhanced by stimulation-dependent dephosphorylation in nerve terminals. *J Biol Chem* 274: 3257–3260.
18. Warren G (1993) Membrane partitioning during cell division. *Annu Rev Biochem* 62: 323–348.
19. Warren G (1985) Membrane traffic and organelle division. *Trends Biochem Sci* 10: 439–443.
20. Royle SJ (2011) Mitotic moonlighting functions for membrane trafficking proteins. *Traffic* 12:791–798.
21. Scita G, Di Fiore PP (2010) The endocytic matrix. *Nature* 463:464–473.
22. Boucrot E, Kirchhausen T (2007) Endosomal recycling controls plasma membrane area during mitosis. *Proc Natl Acad Sci USA* 104:7939–7944.
23. Boucrot E, Kirchhausen T (2008) Mammalian cells change volume during mitosis. *PLoS ONE* 3:e1477.
24. Chetrit D, et al. (2011) Negative regulation of the endocytic adaptor disabled-2 (Dab2) in mitosis. *J Biol Chem* 286:5392–5403.
25. Fürthauer M, González-Gaitán M (2009) Endocytosis and mitosis: A two-way relationship. *Cell Cycle* 8:3311–3318.
26. Neto H, Collins LL, Gould GW (2011) Vesicle trafficking and membrane remodelling in cytokinesis. *Biochem J* 437:13–24.
27. Grant BD, Donaldson JG (2009) Pathways and mechanisms of endocytic recycling. *Nat Rev Mol Cell Biol* 10:597–608.
28. Kozik P, Francis RW, Seaman MN, Robinson MS (2010) A screen for endocytic motifs. *Traffic* 11:843–855.
29. Nilsson T, Jackson M, Peterson PA (1989) Short cytoplasmic sequences serve as retention signals for transmembrane proteins in the endoplasmic reticulum. *Cell* 58: 707–718.
30. Seaman MN (2004) Cargo-selective endosomal sorting for retrieval to the Golgi requires retromer. *J Cell Biol* 165:111–122.
31. Seaman MN (2007) Identification of a novel conserved sorting motif required for retromer-mediated endosome-to-TGN retrieval. *J Cell Sci* 120:2378–2389.
32. Lobel P, Fujimoto K, Ye RD, Griffiths G, Kornfeld S (1989) Mutations in the cytoplasmic domain of the 275 kd mannose 6-phosphate receptor differentially alter lysosomal enzyme sorting and endocytosis. *Cell* 57:787–796.
33. Lin SX, Mallet WG, Huang AY, Maxfield FR (2004) Endocytosed cation-independent mannose 6-phosphate receptor traffics via the endocytic recycling compartment en route to the trans-Golgi network and a subpopulation of late endosomes. *Mol Biol Cell* 15:721–733.
34. Vassilev LT, et al. (2006) Selective small-molecule inhibitor reveals critical mitotic functions of human CDK1. *Proc Natl Acad Sci USA* 103:10660–10665.
35. Heuser JE, Anderson RG (1989) Hypertonic media inhibit receptor-mediated endocytosis by blocking clathrin-coated pit formation. *J Cell Biol* 108:389–400.
36. Royle SJ, Bright NA, Lagnado L (2005) Clathrin is required for the function of the mitotic spindle. *Nature* 434:1152–1157.
37. Liu L, Shi H, Chen X, Wang Z (2011) Regulation of EGF-stimulated EGF receptor endocytosis during M phase. *Traffic* 12:201–217.
38. Mills IG (2007) The interplay between clathrin-coated vesicles and cell signalling. *Semin Cell Dev Biol* 18:459–470.
39. Habela CW, Sontheimer H (2007) Cytoplasmic volume condensation is an integral part of mitosis. *Cell Cycle* 6:1613–1620.
40. Stewart MP, et al. (2011) Hydrostatic pressure and the actomyosin cortex drive mitotic cell rounding. *Nature* 469:226–230.
41. Coupin GT, Muller CD, Rémy-Kristensen A, Kuhry JG (1999) Cell surface membrane homeostasis and intracellular membrane traffic balance in mouse L929 cells. *J Cell Sci* 112:2431–2440.
42. Erickson CA, Trinkaus JP (1976) Microvilli and blebs as sources of reserve surface membrane during cell spreading. *Exp Cell Res* 99:375–384.
43. Follett EA, Goldman RD (1970) The occurrence of microvilli during spreading and growth of BHK21-C13 fibroblasts. *Exp Cell Res* 59:124–136.
44. Kunda P, Baum B (2009) The actin cytoskeleton in spindle assembly and positioning. *Trends Cell Biol* 19:174–179.
45. Devenport D, Oristian D, Heller E, Fuchs E (2011) Mitotic internalization of planar cell polarity proteins preserves tissue polarity. *Nat Cell Biol* 13:893–902.

Supporting Information

Fielding et al. 10.1073/pnas.1117401109

SI Materials and Methods

Cell Culture and Reagents. HeLa cells were grown in DMEM containing 10% (vol/vol) FBS and penicillin/streptomycin at 37°C and 5% CO_2. Transfections were carried out according to manufacturer's instructions by using either GeneJuice (Novagen) or Lipofectamine 2000 (Invitrogen). The CD8-chimera constructs (1) were a kind gift from Scottie Robinson (University of Cambridge, Cambridge, United Kingdom).

The amino acid sequences of the latter parts of CD8 proteins were as follows:

CD8-WT KRLKRRRVCKCPRPVVKSGDKPSLSARYV*
CD8-CIMPR KRLKYKKERREMVMSRLTNCCRRSANVSY
KYSKVNKEEEADENETEWLMEEIQPPAPR
PGKEGQENGHVAAKSVRAADTLSALHGDE
QDSEDEVLTLPEVKVRPPGRAPGAEGGPP
LRPLPRKAPPPLRADDRVGLVRGEPARRG
RPRAAATPISTFHDDSDEDLLHV*
CD8-8xA KRLKRRRIPAAAAAAAAV*
CD8-YAAL KRLKRRRIPAAYAALAAV*
CD8-EAAALL KRLKRRRIPAEAAALLAV*
CD8-FANPAY KRLKRRRIPAFANPAYAV*

H2B-GFP, H2B-mCherry, and GFP-LCa were available from previous work (2). Mouse monoclonal anti-clathrin heavy chain antibody was purified from hybridoma CRL-2228 (ATCC). All reagents were from Sigma, unless stated otherwise.

Flow Cytometry. Analysis of surface and internalized CD8 was performed as described (1). Briefly, HeLa cells expressing CD8 constructs were synchronized in S phase with 2 mM thymidine for 18 h, at the G_2/M checkpoint with 9 μM RO-3306 for 18 h (3) and in M-phase either by 30-min release from RO-3306 treatment or with 40 ng/mL nocodazole for 16 h. Thymidine and RO-3306 arrested cells were trypsinized, whereas cells in mitosis (nocodazole-arrested or those released for 30 min from RO-3306 block) were gently isolated by shake off. We estimate that interphase-synchronized cell populations and (after shake off) mitotic populations were >99% pure. Cells were then centrifuged at 4,000 × *g* for 5 min and resuspended in growth medium containing mouse anti-human CD8 Alexa488-conjugated antibody (1:50, MCA1226A488; Serotec) at 37 °C for 40 min to allow internalization. Subsequently, cells were washed in ice-cold 1% (wt/vol) BSA/PBS before incubation with rabbit anti-Alexa488 (1:67, A11094; Invitrogen) and anti-mouse IgG Alexa633-conjugated secondary antibodies (1:200; Invitrogen), at 4 °C for 30 min. Cells were then washed and fixed in 3.7% (wt/vol) paraformaldehyde before analysis by flow cytometry (FACSCalibur; Becton Dickinson). For quantification of internalized anti-CD8 Alexa488, cells expressing equivalent amounts of surface CD8 construct were gated, as described (1). The gate was a rectangle that spanned the *x* axis and excluded the nontransfected cells and those with very high amounts of CD8 on the surface (20–200 a.u. in Fig. 1*C*). As a control representing endocytic block, interphase cells were incubated with hypertonic sucrose (0.45 M) during the uptake assay (4). For each condition, 1×10^4 cells were measured and after gating, $>1 \times 10^3$ events were analyzed. This number is far in excess of the tens of cells analyzed by light microscopy in previous studies (5).

For analysis of transferrin uptake, synchronized cells were trypsinized or isolated by shake off and starved for 30 min in serum-free media. Cells were then incubated with 50 μg/mL Alexa488-conjugated transferrin for 5 min at 4 °C, then moved to 37 °C and incubated for 10 min. Cells were pelleted, washed in ice cold 1% (wt/vol) BSA/PBS, acid-washed twice, and fixed before flow cytometric analysis. For surface bound and internalized transferrin analysis cells were incubated with Alexa488-labeled transferrin as described above. After an acid wash, cells were resuspended in ice cold 1% (wt/vol) BSA/PBS containing 50 μg/mL Alexa647-conjugated transferrin (Invitrogen) and incubated for 30 min on ice. Cells were then washed, fixed, and analyzed by flow cytometry. For each sample, 1×10^4 events from each sample were acquired, and geometric means from four independent experiments were used for comparison and statistical analysis.

Analysis of internalized and surface transferrin receptor (TfR) was performed by using a similar method to CD8 labeling. HeLa cells were synchronized with thymidine, RO-3306 (10 μM), or nocodazole for 18 h. After synchronization, cells were harvested appropriately (cells synchronized in M phase by using RO-3306 were released for 60 min from the drug treatment), centrifuged, and resuspended in growth medium containing mouse anti-human TfR-FITC conjugated antibody (1:5, SAB4700518; Sigma-Aldrich). Samples were preincubated on ice for 20 min to allow antibody binding to the surface receptors before transfer to 37 °C for 20 min for the internalization to occur. Control (4 °C) samples were not transferred to 37 °C but kept on ice. As a control representing endocytic block, thymidine-treated cells were incubated with hypertonic sucrose (0.5 M) during the 37 °C uptake assay. After incubation with the antibody, cells were washed in ice-cold 1% BSA/PBS, before incubation with rabbit anti-FITC (1:50, 71–1900; Invitrogen) and anti-mouse IgG Alexa633-conjugated antibodies at 4 °C for 30 min. Cells were then washed, fixed, and analyzed by flow cytometry. For each sample, 1×10^4 events were acquired and geometric means with no gating from three independent experiments were used for comparison and statistical analysis.

Immunofluorescence and Live-Cell Labeling. HeLa cells on glass coverslips were fixed with 3% paraformaldehyde and 4% sucrose in PBS (wt/vol). For steady-state localization of CD8 constructs, cells were permeabilized with 0.5% Triton X-100 in PBS (vol/vol) for 10 min. For staining of surface transferrin receptor, no permeabilization was carried out. Cells were blocked [3% (wt/vol) BSA and 5% (vol/vol) goat serum in PBS] before addition of primary antibodies, followed by washing and secondary antibody incubation (where necessary). Finally, cells were washed and mounted in Mowiol containing 10 μg/mL 4′,6-diamidino-2-phenylindole (DAPI).

For immunofluorescence analysis of the CD8 uptake assay, cells were prepared and stained as above except cells were grown on coverslips with no synchronization and anti-mouse IgG Alexa568-conjugated secondary antibody was used.

For live-cell imaging of CD8 uptake, cells were cotransfected with H2B-mCherry and the CD8 constructs. Cells were synchronized by using RO-3306 as above, released for 25 min, then transferred to CO_2-independent media and a 37 °C, humidified microscope chamber (Okolab S.r.l). Cells in prometaphase or metaphase were identified by H2B-mCherry. Alexa488-conjugated anti-CD8 antibody was then added at 1:100 dilution in CO_2-independent media, and images were acquired every 30 s for 30 min.

For transferrin uptake experiments, the cells were incubated for 45 min at 37 °C in serum-free DMEM. Cells were first incubated on ice for 5 min followed by addition of 50 μg/mL Alexa488-conjugated transferrin (Invitrogen) in serum-free me-

dia. After 30 min on ice, cells were transferred to a 37°C/5% CO_2 incubator for 7 min (adequate time to allow substantial uptake but sufficiently short so that cells are unlikely to have progressed significantly through the cell cycle during the course of the uptake). Cells were then acid-washed (0.1 M glycine and 150 mM NaCl, pH 3) to remove surface-bound transferrin before fixation (3% paraformaldehyde and 4% sucrose in PBS) for 15 min. Subsequently, cells were processed for immunofluorescence as above and stained with rabbit anti-transferrin receptor (CBL47; Chemicon) followed by anti-rabbit Alexa568 secondary antibody (1:500; Invitrogen).

For FM4-64 uptake experiments, HeLa cells transiently expressing H2B-GFP were incubated with FM4-64 (15 μM; Invitrogen) for 10 min. Excess dye was washed from the plasma membrane by using normal extracellular solution (136 mM NaCl, 2.5 mM KCl, 1.3 mM $MgCl_2$, 10 mM Hepes, 2 mM $CaCl_2$, and 10 mM glucose at pH 7.4) for 10 min.

Microscopy. Microscopy was performed on a Leica confocal microscope SP2 with a 63× (1.4 N.A.) oil-immersion objective. Alexa488 and Alexa568 were excited by using Ar/Kr 488 nm or He/Ne 543 nm laser lines, respectively. DAPI was excited by using a multiphoton laser. Excitation and collection of emission were performed separately and sequentially. *Z*-series were acquired by using the software's optimized z-depth between each slice (0.122 μm). For live-cell experiments, either a Nikon Ti fluorescence microscope and DS-Qi 1Mc camera (CD8 experiments) or an Olympus IX81 fluorescence microscope and Orca-ER camera (FM dye experiments) was used with a 60× oil-immersion objective.

Data Analysis. Flow cytometry data were analyzed, plots were generated in CellQuest (Becton Dickinson), and histograms were made in WinMDI. Quantification of transferrin uptake and surface transferrin receptor from confocal *Z*-series was performed in Image J by thresholding the stack, drawing around cell outlines, and measuring each section. The background-corrected mean intensities for all slices were summed to give the total intensity for each cell. Alternative methods of quantification produced the same result. Image J was used to create the maximum intensity projections shown in supporting information. Data were plotted in Igor Pro-6.2 (Wavemetrics). Figures were assembled in Adobe Photoshop. For statistical testing, one-way ANOVA with Tukey's or Dunnett's post hoc test was used to compare multiple groups. Where only two groups were compared, Student's *t* test was used in Instat (GraphPad).

1. Kozik P, Francis RW, Seaman MN, Robinson MS (2010) A screen for endocytic motifs. *Traffic* 11:843–855.
2. Royle SJ, Bright NA, Lagnado L (2005) Clathrin is required for the function of the mitotic spindle. *Nature* 434:1152–1157.
3. Vassilev LT, et al. (2006) Selective small-molecule inhibitor reveals critical mitotic functions of human CDK1. *Proc Natl Acad Sci USA* 103:10660–10665.
4. Heuser JE, Anderson RG (1989) Hypertonic media inhibit receptor-mediated endocytosis by blocking clathrin-coated pit formation. *J Cell Biol* 108:389–400.
5. Boucrot E, Kirchhausen T (2007) Endosomal recycling controls plasma membrane area during mitosis. *Proc Natl Acad Sci USA* 104:7939–7944.

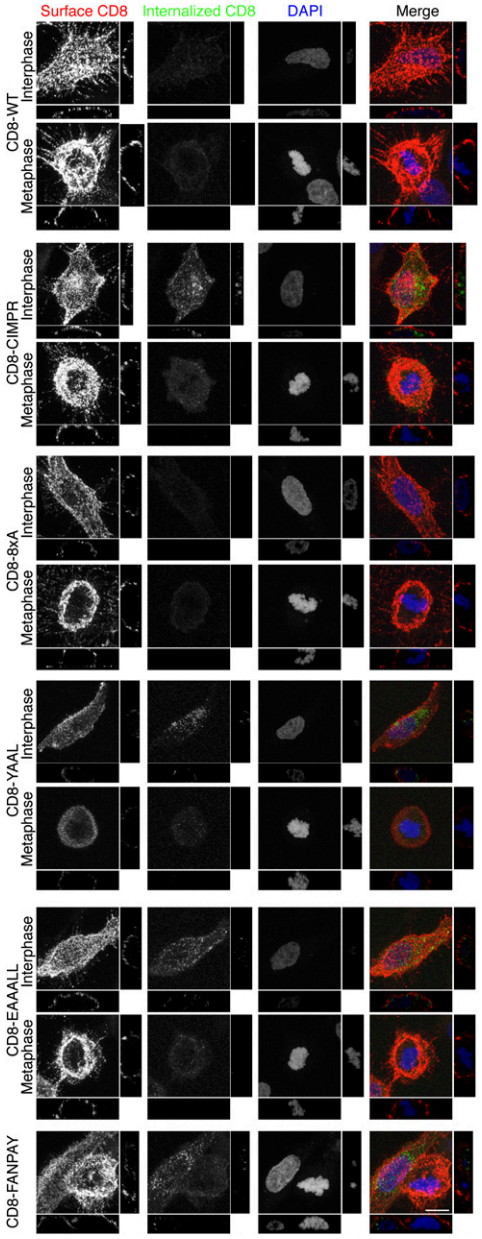

Fig. S1. Mitotic inhibition of endocytosis: CD8 trafficking in interphase or early mitotic cells. 3D confocal reconstructions of representative cells expressing each CD8 construct. A maximum intensity projection of a confocal *Z*-series is shown en face (*x-y*) or as *y-z* and *x-z* orthogonal sections for each channel. (Scale bar: 10 μm.)

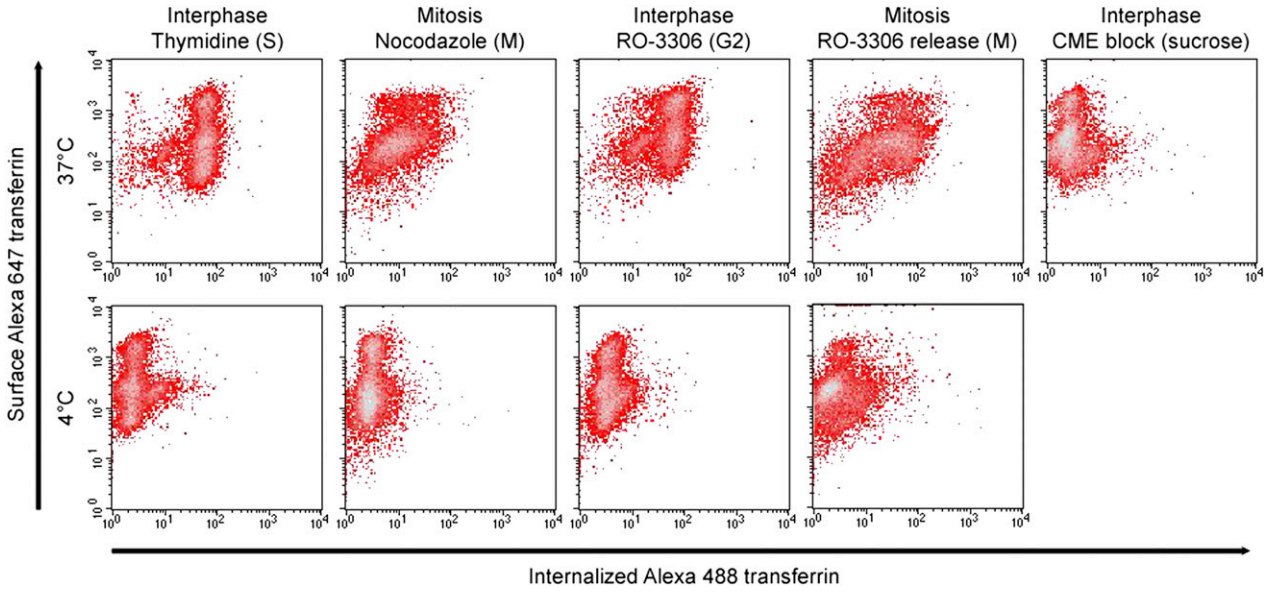

Fig. S2. Transferrin uptake is inhibited during early mitosis despite abundant surface TfR. Quantification of transferrin uptake and surface transferrin by flow cytometry. Results from a single experiment are shown. Plots of internalized versus surface transferrin are shown. Note that there is (*i*) no decrease in the amount of surface transferrin in any condition and (*ii*) the leftward shift of the plots from mitotic cells. Plots are pseudocolored to show the density of points.

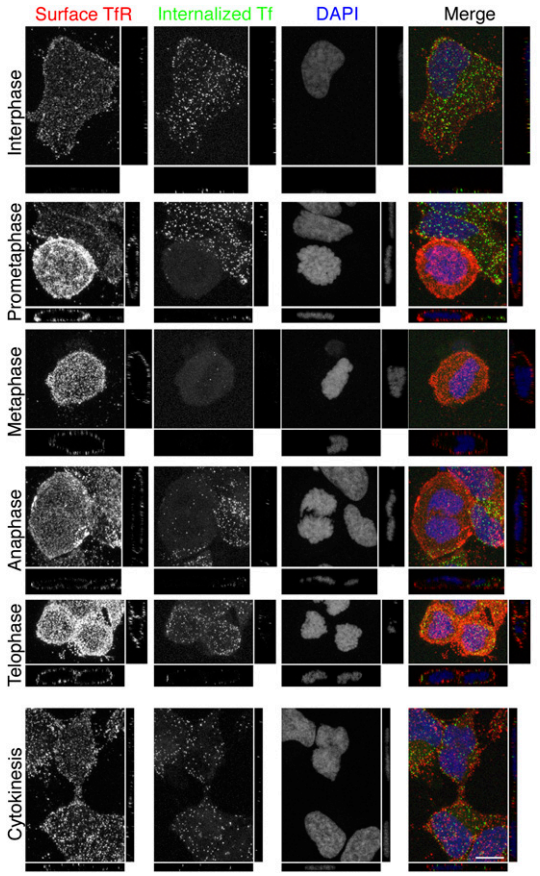

Fig. S3. Transferrin uptake is inhibited during early mitosis despite abundant surface TfR. 3D confocal reconstructions of the cells that are shown in Fig. 4. A maximum intensity projection of a confocal *Z*-series is shown en face (*x-y*) or as *y-z* and *x-z* orthogonal sections for each channel. (Scale bar: 10 μm.)